A Mechanistic Study of the Cycloaddition−Cycloreversion Reactions of the Zirconium−Imido Complex $Cp_2Zr(N\text{-}t\text{-}Bu)(THF)$ with Organic Imines and Azides

Karen E. Meyer, Patrick J. Walsh, and Robert G. Bergman*

Department of Chemistry, University of California, Berkeley, California 94720

Received August 31, 1994[⊗]

Abstract: Treatment of $Cp_2Zr(=N\text{-}t\text{-}Bu)(THF)$ (**1**) with benzaldehyde phenylimine (**4**) at room temperature gives 2,4-diaza-1-zirconacyclobutane (**2**) in high yield. This complex reacts further with additional imine to give N-*tert*-butylphenylimine (**5**) and diazazirconacyclobutane **3**. The latter reaction, an imine metathesis, was subjected to a detailed kinetic study. The observed saturation kinetic behavior established that the first step in the reaction involves reversible apparent [2 + 2] retrocycloaddition of diazametallacycle **2** to give imine **5** and the transient intermediate $Cp_2ZrN{=}Ph$ (**6**). The transient imido species is then trapped by an analogous cycloaddition reaction with imine **4** to give **3**. Supporting evidence for this mechanistic picture was provided by a parallel kinetic study of the reaction of diazametallacycle **2** with diphenylacetylene and 2-butyne. These reactions give azazirconacyclobutenes **7a** and **7b** by a reaction that is first order in **2** and zero order in alkyne. The fact that the saturation rate constants measured in these reactions are identical to the one observed in the imine metathesis provides strong evidence that the same intermediate, $Cp_2Zr{=}NPh$, is involved in all three reactions. Competition and equilibration studies provided data sufficient to construct a complete free energy diagram for the interconversion of azametallacycles **2** and **3** with one another and with azametallacyclobutene **7b**. Imido complex **1** also undergoes [3 + 2] cycloaddition reactions with *tert*-butyl, phenyl, and *p*-tolyl azides, leading to metallatetrazenes **8**, **9a**, and **9b**. The structure of **8** was determined by X-ray diffraction (crystal data: space group: $P2_12_12_1$; a = 8.5618(13) Å, b =14.4507(18) Å, c = 15.1037(17) Å; $Z = 4$; $R = 5.1$; $R = 4.8\%$; $R_w = 6.6\%$). These materials undergo extrusion of tert-butyl azide at 45 °C, followed by reaction with additional azide to give tetrazene complexes **10a** and **10b**. Trapping studies with imines and bicyclo-[2.2.1]hept-2-ene provide evidence that the first phase of the azide metathesis involves retro[3 + 2]cycloaddition, extruding $t\text{-}BuN_3$ to give $Cp_2Zr{=}NPh$, followed by reaction of the latter species with additional azide. Attempts to trap $Cp_2Zr{=}NPh$ with alkynes in the presence of azide led to new complexes **13** and **14**. The structure of **14** was determined by X-ray diffraction (crystal data: space group: $P2_1/n$; a = 9.927(2) Å, b = 13.377(2) Å, c = 18.068(3) Å; $\alpha = 90.0°$, $\beta = 97.605(14)°$, $\gamma = 90.0°$; $Z = 4$; $R = 13.6$; $R = 7.2\%$, $R_w = 8.3\%$). Spectroscopic monitoring and control reactions demonstrated that these materials arise by initial formation of azametallacyclobutenes, followed by reaction of the latter materials with organic azide.

Introduction

Extensive research efforts have focused recently on transition-metal complexes that contain multiply bonded ligands.[1,2] Perhaps the most compelling argument for work in this area is the number of important chemical reaction processes that involve such complexes.[3] We have been interested in the monomeric group IV transition-metal oxo,[4−6] imido,[7−16] and sulfido[5,6] complexes. Monomeric compounds that contain reactive M = X bonds are rare.[8,11,17] Some complexes in this series exhibit a rich reaction chemistry that gives rise to the formation of new C−X (X = O, NR, S) bonds.[4,5,7−10,18−20] This report focuses on imidozirconium complexes and specifically details the role of $Cp_2Zr(=NR)$ in overall [2 + 2] (eq 1) and [3 + 2] (eq 2) cycloaddition/cycloreversion reactions.

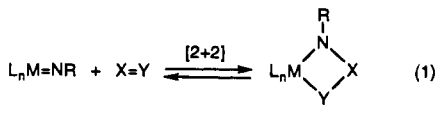

(1)

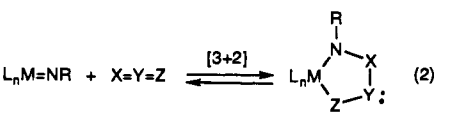

(2)

Imidozirconium complexes having the general structure $Cp_2Zr(=NR)$ undergo reactions with unsaturated organic molecules to give formal [2 + 2] cycloaddition products. For instance, reactions are observed with some alkenes (R = *t*-Bu) and many

[⊗] Abstract published in *Advance ACS Abstracts*, December 15, 1994.

(1) Collman, J. P.; Hegedus, L. S.; Norton, J. R.; Finke, R. G. *Principles and Applications of Organotransition Metal Chemistry*; University Science Books: Mill Valley, 1987.
(2) Nugent, W. A.; Mayer, J. A. *Metal-Ligand Multiple Bonds*; Wiley-Interscience: New York, 1988.
(3) Dragutan, V.; Balban, A. T.; Dimonie, M. *Olefin Metathesis and Ring Opening Polymerization of Cyclo-Olefins*; Wiley-Interscience: Chichester, 1985.
(4) Camey, M. J.; Walsh, P. J.; Hollander, F. J.; Bergman, R. G. *J. Am. Chem. Soc.* **1989**, *111*, 8751.
(5) Camey, M. J.; Walsh, P. J.; Bergman, R. G. *J. Am. Chem. Soc.* **1990**, *112*, 6426.
(6) Howard, W. A.; Parkin, G. *J. Am. Chem. Soc.* **1994**, *116*, 606.
(7) Walsh, P. J.; Hollander, F. J.; Bergman, R. G. *J. Am. Chem. Soc* **1988**, *110*, 8729.
(8) Walsh, P. J.; Hollander, F. J.; Bergman, R. G. *Organometallics* **1993**, *12*, 3705.
(9) Cummins, C. C.; Baxter, S. M.; Wolzanski, P. T. *J. Am. Chem. Soc.* **1988**, *110*, 8731.
(10) Cummins, C. C.; Schaller, C. P.; Vanduyne, G. D.; Wolczanski, P. T.; Chan, A. W. E.; Hoffmann, R. *J. Am. Chem. Soc.* **1991**, *113*, 2985.
(11) Arney, D. J.; Bruck, M. A.; Huber, S. R.; Wigley, D. E. *Inorg. Chem.* **1992**, *31*, 3749.
(12) Hill, J. E.; Profilet, R. D.; Fanwick, P. E.; Rothwell, I. P. *Angew. Chem., Int. Ed. Eng.* **1990**, *29*, 664.
(13) Hill, J. E.; Fanwick, P. E.; Rothwell, I. P. *Inorg. Chem.* **1991**, *30*, 1143.

0002-7863/95/1517-0974$09.00/0

Scheme 1

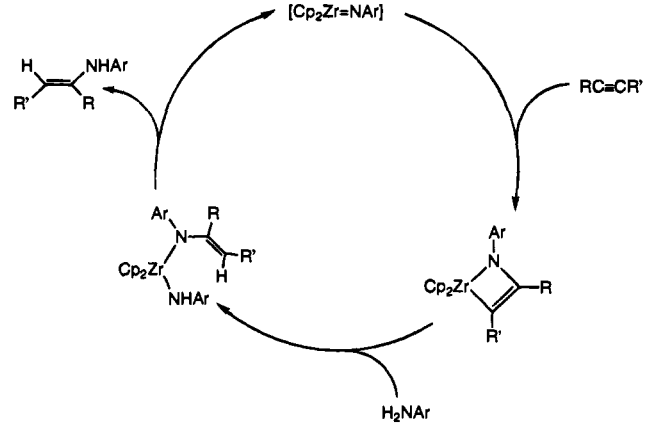

alkynes (R = *t*-Bu, 2,6-dimethylphenyl) to yield four-membered azametallacyclobutanes or -butenes.[7,8] A catalytic hydroamination reaction was developed for which kinetic and mechanistic studies confirmed the intermediacy of imidozirconium as well as azametallacyclobutene intermediates (Scheme 1).[18] Other unsaturated organic molecules, including aldehydes[8] and imines,[21] were also found to react with the imido complex.

While [3 + 2] cycloaddition reactions of imidozirconium complexes have not been studied before, examples of metal imido complexes undergoing such reactions are known.[22,23] Addition of organic azides to the osmium imido complex (*p*-cymene)Os=N-*t*-Bu generates a series of tetraazametallacyclopentene (tetrazene) complexes (eq 3).[24] The intermediacy of transient imido species has also been proposed in the formation of other tetrazene complexes.[23] A related observation in the main group, the reaction of $Me_2Si(t\text{-}BuN)_2Ge$ with $TolN_3$,[25] also probably proceeds via an imido intermediate (eq 4).

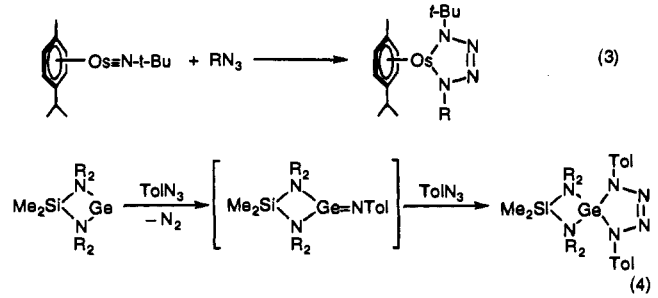

There are only a few examples of metathesis reactions that involve imido complexes; alkylidene complexes are known to react with imines to give metal imido products with release of an alkene.[26,27] There have also been reports of carbodiimide metathesis reactions proposed to involve metal imido intermediates.[28–30] In a preliminary report, we described the stoichiometric zirconium-mediated imine metathesis reaction illustrated in eqs 5 and 6.[21] To determine whether imido complex **1** will also undergo [3 + 2] cycloadditions, we have now investigated its reactions with organic azides. Addition occurs rapidly to give tetraazazirconacyclopentene complexes. In contrast to the stability of most mid and late transition-metal tetrazenes, those obtained from **1** and organic azides are more reactive, undergoing unprecedented retro[3 + 2]cycloreversion that eliminates a different molecule of azide. Contained in this report is a full account of the zirconium-mediated imine metathesis reaction and our findings on the related azide metathesis transformations.

Results

Imine Metathesis Reaction. Treatment of $Cp_2Zr(=N\text{-}t\text{-}Bu)(THF)$[21] (**1**) with benzaldehyde *N*-phenylimine at room temperature in toluene solution immediately gave the red 2,4-diazametallacyclobutane product **2** in 91% yield (eq 5). Thermolysis of **2** at 85 °C with 1 equiv of the imine **4** resulted in stoichiometric metathesis that produced benzaldehyde *N*-*tert*-butylimine (**5**) and the new purple diazametallacycle **3** in 93% yield (eq 6). In the absence of excess imine, both **2** and **3** are stable toward cycloreversion at 25 °C but undergo elimination of imine (**5** in the case of **2** and **4** in the case of **3**) at elevated temperatures to give dimeric $[Cp_2Zr(NPh)]_2$ (eq 7).[21,31]

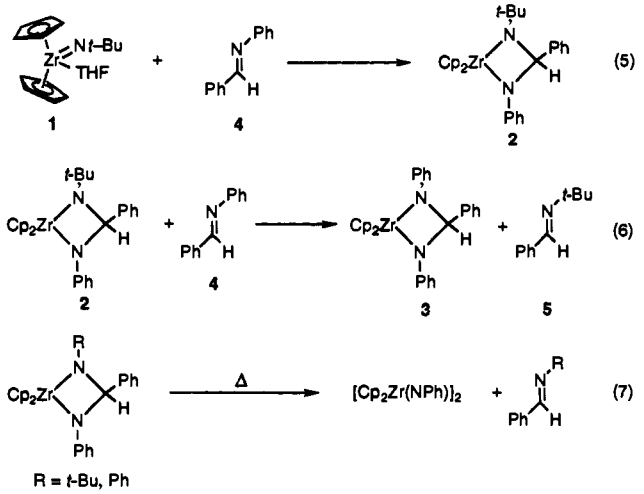

The proposed mechanism of the imine metathesis reaction is included in Scheme 2. In order to verify that this occurs by a dissociative process, kinetic studies were carried out on the reaction of metallacycle **2** with imine **4** in the presence of added imine **5** and excess concentrations of both imines, used to maintain pseudo-first order rate behavior for **2**. Solutions were prepared in toluene or toluene-d_8. The disappearance of the starting metallacycle was monitored at 70 °C, and reactions were followed for >3.5 half-lives. Rate data obtained by ^1H NMR

(14) Profilet, R. D.; Zambrano, C. H.; Fanwick, P. E.; Nash, J. J.; Rothwell, I. P. *Inorg. Chem.* **1990**, *29*, 4363.
(15) Bai, T.; Roesky, H. W.; Noltemeyer, M. Z. *Anorg. Allg. Chem.* **1991**, *595*, 21.
(16) Bai, Y.; Noltemeyer, M.; Roesky, H. W. Z. *Naturforsch* **1991**, *46b*, 1357.
(17) Cardin, D. J.; Lappert, M. F.; Raston, C. L. *Chemistry of Organozirconium and -hafnium Compounds*; Ellis Horwood Limited: Chichester, 1986.
(18) Baranger, A. M.; Walsh, P. J.; Bergman, R. G. *J. Am. Chem. Soc.* **1993**, *115*, 2753.
(19) McGrane, P. L.; Livinghouse, T. *J. Org. Chem.* **1992**, *57*, 1323.
(20) McGrane, P. L.; Jensen, M.; Livinghouse, T. *J. Am. Chem. Soc.* **1992**, *114*, 5459.
(21) Meyer, K. E.; Walsh, P. J.; Bergman, R. G. *J. Am. Chem. Soc.* **1994**, *116*, 2669.
(22) Jung, J. H.; Lee, S. W. *Bull. Kor. Chem. Soc.* **1993**, *14*, 1.
(23) Trogler, W. C. *Acc. Chem. Res.* **1990**, *23*, 426 and references therein.
(24) Michelman, R. I.; Andersen, R. A.; Bergman, R. G. *Organometallics* **1993**, *12*, 2741.
(25) Klein, B.; Neumann, W. P. *J. Organomet. Chem.* **1994**, *465*, 119.
(26) Rocklage, S. M.; Schrock, R. R. *J. Am. Chem. Soc.* **1980**, *102*, 7808.
(27) Rocklage, S. M.; Schrock, R. R. *J. Am. Chem. Soc.* **1982**, *104*, 3077.
(28) Birdwhistell, K. R.; Boucher, T.; Ensminger, M.; Harris, S.; Johnson, M.; Toporek, S. *Organometallics* **1993**, *12*, 1023.
(29) Birdwhistell, K. R.; Gross, R.; Harris, S.; Toporek, S. In *Abstracts, 206th National Meeting of the American Chemical Society*; Chicago, IL, August, 1993.
(30) Meisel, I.; Hertel, G.; Weiss, J. *J. Mol. Catal.* **1986**, *36*, 159.
(31) Latesky, S. L.; McMullen, A. K.; Niccolai, G. P.; Rothwell, I. P.; Huffman, J. C. *Organometallics* **1985**, *4*, 1896.

Scheme 2

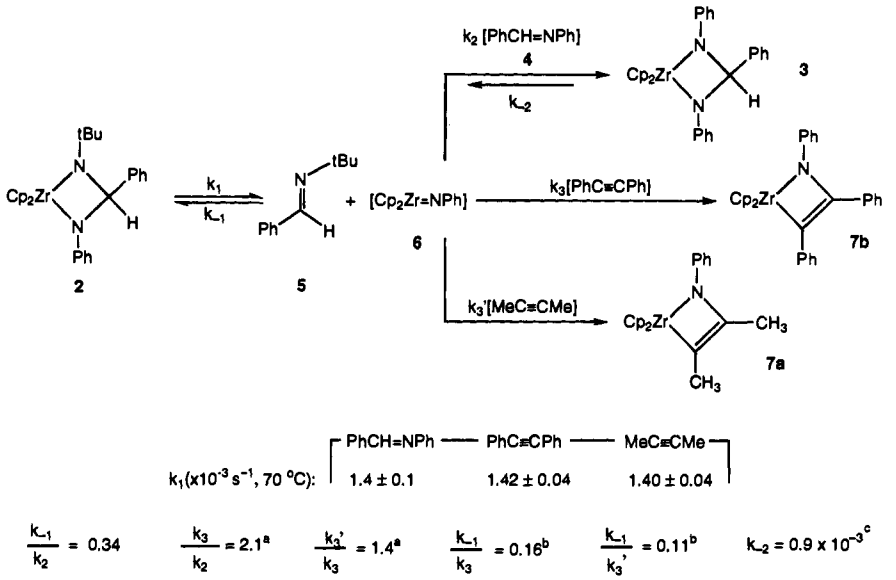

[a] From competition studies. [b] Calculated from experimentally measured rate constant ratios. [c] Determined from rate of reaction of diazametallacycle **3** with excess PhC≡CPh.

Table 1. Concentration and Rate Data for the Reaction of Zirconacyclobutane **2** with Benzaldehyde *N*-Phenylimine at 70 °C in toluene

[2] (×10³ M)	[5] (×10² M)	[4] (×10² M)	k (×10³ s⁻¹)
3.33	2.04	5.18	1.14
3.33	2.72	5.18	1.15
3.33	1.70	5.18	1.22
3.33	1.36	5.18	1.27
3.33	1.02	5.18	1.23
3.33	4.10	5.18	1.12
3.33	6.16	5.18	1.02
3.33	4.74	5.18	1.05
3.33	2.28	16.4	1.29
3.33	2.28	20.5	1.35
3.33	2.28	18.1	1.34
3.33	2.28	11.5	1.22
3.33	2.28	45.9	1.40
3.33	2.28	36.6	1.42
4.44	2.65	25.2	1.38[a]
4.44	2.65	12.6	1.22[a]
7.07	7.75	53.8	1.43[a]

[a] These runs carried out by ^{1}H NMR spectroscopy in toluene-d_8; all others monitored by UV–vis spectroscopy.

and UV–vis spectrometry for identical sample solutions were in good experimental agreement.

Conditions for the kinetic experiments are discussed in the Experimental Section. Excellent pseudo first-order behavior was observed; Table 1 contains the concentration and rate data. As noted below, the conversion of **2** to **3** is reversible. Under most of the conditions used for the kinetic experiments a relatively high ratio of [**4**] to [**5**] was maintained (Table 1). The combination of this and the modestly negative standard free energy of the reaction insured that the overall back reaction was sufficiently slower than the forward reaction to allow us to ignore it in the kinetic analysis (*vide infra*). In order to check this, however, for the first eight runs listed in Table 1 (where the concentrations of added imines **4** and **5** are comparable) we computed rate constants using data taken for approximately the first 30% of conversion of **2** to **3**. These "initial rate" values were within experimental error of those calculated using the full data sets.

Plots of the decrease in [**2**] versus time gave exponential decay consistent with the reaction being first order in [**2**]. Rates measured using variable concentrations of both **4** and **5** demonstrated that at low concentrations of entering imine **4** the rate was accelerated by added **4** and inhibited by extruded imine **5**. A plot of k_{obs} versus [**4**]/[**5**] was obtained (Figure 1) that clearly illustrates saturation kinetics at higher concentrations of *N*-phenylimine **4**. A plot of $1/k_{obs}$ versus [**5**]/[**4**] (see inset Figure 1), although somewhat scattered, shows an essentially linear dependence on the imine ratio.

$$\text{rate} = \frac{k_1 k_2 [\mathbf{2}][\mathbf{4}]}{k_{-1}[\mathbf{5}] + k_2[\mathbf{4}]} = k_{obs}[\mathbf{2}] \tag{8a}$$

$$\frac{1}{k_{obs}} = \frac{k_{-1}}{k_1 k_2}\frac{[\mathbf{5}]}{[\mathbf{4}]} + \frac{1}{k_1} \tag{8b}$$

$$K_{eq} = \frac{[\mathbf{3}]_{eq}[\mathbf{5}]_{eq}}{[\mathbf{2}]_{eq}[\mathbf{4}]_{eq}} \tag{9}$$

These data are consistent with a dissociative mechanism and the rate law given in eqs 8a and 8b. Values of $k_1 = 1.4 \pm 0.1 \times 10^{-3}$ s^{-1} and $k_{-1}/k_2 = 0.32 \pm 0.02$ were derived from the inverse first-order plot. Following the kinetic study, the concentration of **5** was increased to facilitate the overall back reaction (k_{-2}), and the equilibrium between **2** and **3** was examined by ^{1}H NMR spectroscopy. Under these conditions we observed side reactions that led to small amounts of the dimer $[Cp_2Zr(NPh)]_2$. However, these irreversible processes were slow enough that we were able to determine the equilibrium constant $K_{eq} = 4.6$ at 70 °C for the **2** to **3** interconversion (eq 9).

Kinetic Study of the Alkyne Trapping Reaction. The diazametallacycle **2** also reacted with 2-butyne and diphenylacetylene at 70 °C to give the metallacyclobutene products **7a** and **7b** (Scheme 2). Monitoring these reactions by ^{1}H NMR spectroscopy showed that **7a** and **7b** were formed cleanly in 89% and 92 % yields, respectively. In order to determine whether the proposed dissociative mechanism (Scheme 2) was also involved in azametallacyclobutene formation, kinetic studies were performed. Excess imine and alkyne were used so that these concentrations remained effectively constant. The disappearance of **2** was monitored at 70 °C by ^{1}H NMR and UV–vis spectrometry.

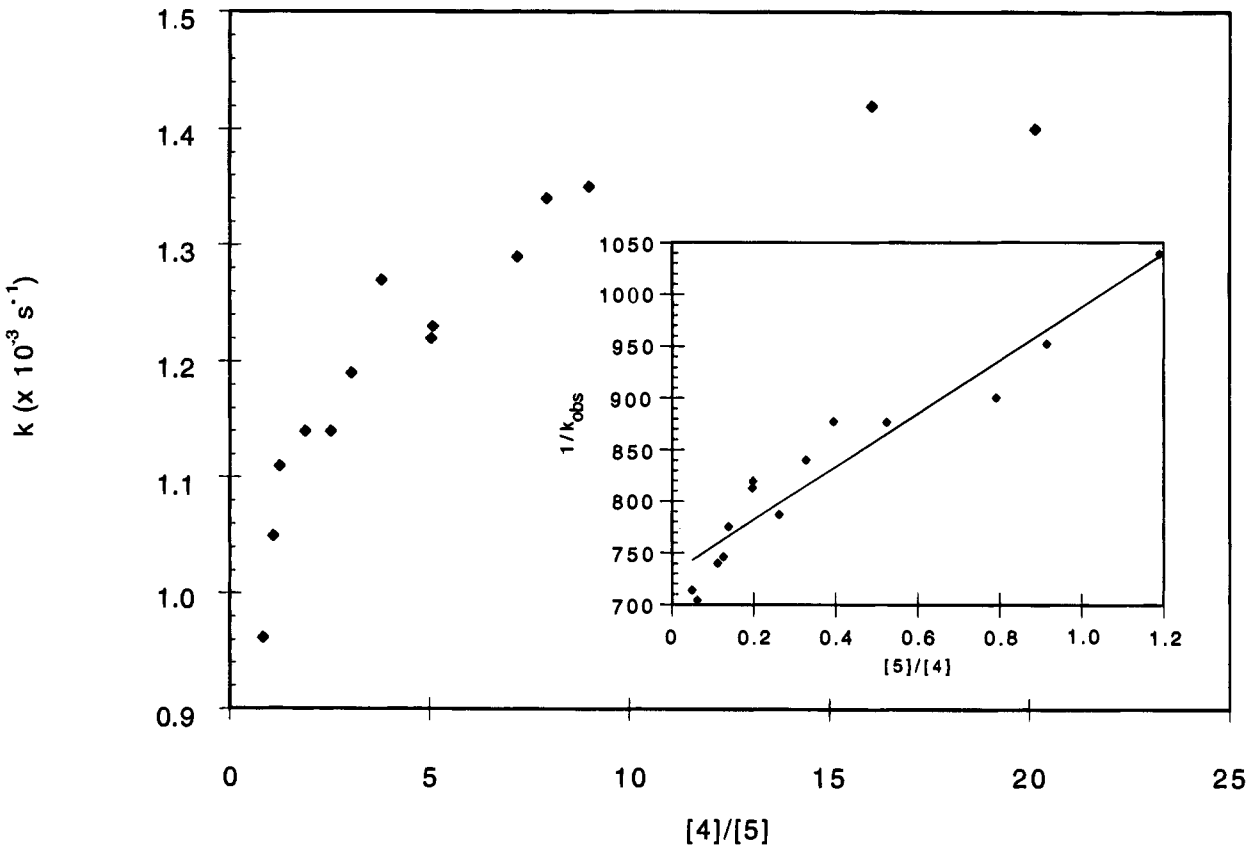

Figure 1. Dependence of k_{obs} for the disappearance of **2** at 70 °C on the concentration of added benzaldehyde *N*-phenylimine (**4**) and reciprocal plot of $1/k_{obs}$ vs [**5**]/[[**4**] (inset). The linear fit gave a correlation coefficient of $\gamma = 0.97$.

Table 2. Concentration and Rate Data for the Reaction of Diazametallacycle **2** with PhC≡CPh ([**2**] = 3.33 × 10^{-3} M; [**5**] = 5.49 × 10^{-2} M)

[PhC≡CPh] (×10^2 M)	k (×10^3 s^{-1})	[PhC≡CPh] (×10^2 M)	k (×10^3 s^{-1})
0.574	1.34	12.2	1.45
0.785	1.39	26.6	1.45
1.89	1.46	36.1	1.46
3.10	1.44	9.12	1.33[a]
6.54	1.42		

[a] This run carried out by NMR spectroscopy; all others monitored by UV–vis spectroscopy. For this experiment only, [**2**] = 3.27 × 10^{-3} M; [**5**] = 5.45 × 10^{-2} M.

Table 3. Concentration and Rate Data for the Reaction of **2** with 2-Butyne[a] ([**2**] = 2.16 × 10^{-3} M; [**5**] = 2.04 × 10^{-2} M)

[MeC≡CMe] (×10^2 M)	k (×10^3 s^{-1})
0.99	1.45
2.78	1.42
4.18	1.42

[a] Concentrations monitored by UV–vis spectroscopy.

A plot of [**2**] versus time gave exponential decay indicative of a pseudo-first-order reaction. The reaction was first order in [**2**] but zero order in [alkyne] even at the lowest concentrations of this reactant that we were conveniently able to reach while still maintaining pseudo-first order conditions in [**2**]. These data (Tables 2 and 3) are consistent with the rate law described in eq 10 (for diphenylacetylene: $k_{obs} = 1.42 \pm 0.04 \times 10^{-3}$ s^{-1}; for 2-butyne: $k_{obs} = 1.43 \pm 0.04 \times 10^{-3}$ s^{-1}). Heating **3** to 70 °C in the presence of diphenylacetylene also gave **7a** in >90% yield by ^{1}H NMR spectroscopy, but more slowly than the complex was formed from **2**. With excess diphenylacetylene, a value of $k_{obs} = 0.90 \pm 0.05 \times 10^{-3}$ s^{-1} was obtained.

$$\text{rate} = k_{obs}[\mathbf{2}] \tag{10}$$

Because k_{-1}/k_3 and k_{-1}/k_3' could not be determined from the alkyne kinetic study due to the inaccessibility of the falloff region, a series of competition experiments were performed. Complex **2** was treated with a mixture of excess imine **4** and diphenylacetylene in toluene-d_8 at 70 °C. The reactions were monitored at early reaction times to determine the kinetic ratio of products **3** and **7a** in this reaction. Measuring the product ratios and dividing out the concentrations gave a value of $k_3/k_2 = 2.1$. Similarly, the reaction of **2** with a mixture of excess 2-butyne and diphenylacetylene was monitored under identical conditions. At early reaction times a ratio of $k'_3/k_3 = 1.4$ was determined. The remaining ratios k_{-1}/k_3 and k_{-1}/k_3' were calculated from the experimentally determined kinetic ratios and k_{-1}/k_2. A summary of the rate constants and ratios measured for this system is included in Scheme 2.

In an effort to probe the catalytic potential of this system, we prepared a solution that contained imines **4**, *p*-anisaldehyde *N*-tolylimine, and 25 mol % of **2** or **3** in toluene-d_8. Heating to 70 °C slowly (turnover no. approximately 0.35 mol imine (mol Zr)$^{-1}$ h^{-1}) gave a statistical mixture of **5**, anisaldehyde *N*-tolylimine, benzaldehyde *N*-tolylimine, and anisaldehyde *N*-phenylimine. The lifetime of the catalyst, however, was limited by the formation of the dimer $[Cp_2Zr(NAr)]_2$.

Cycloaddition of Organoazides. Retrocycloaddition of Tetrazene Complexes. Addition of 1 equiv of *t*-BuN_3 or ArN_3 (Ar = Ph or Tol) to a benzene solution of **1** at 25 °C immediately gave the dark purple [2 + 3] cycloaddition products **8** and **9a,b** in >95% yield by ^{1}H NMR spectrometry (Scheme 3). Surprisingly, at slightly elevated temperatures (45 °C)

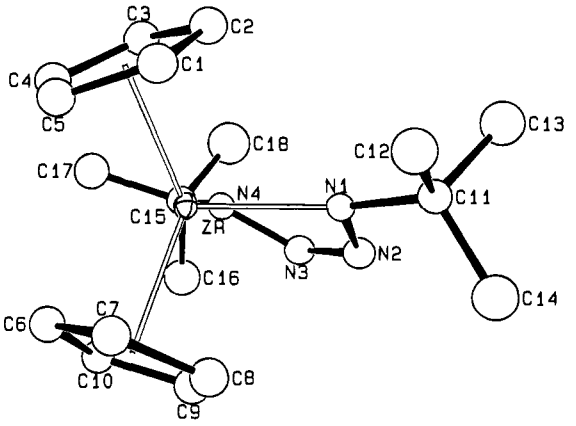

Figure 2. ORTEP diagram illustrating the geometry and labeling scheme for complex **8**. The spheres are scaled to represent the 50% probability surface.

Scheme 3

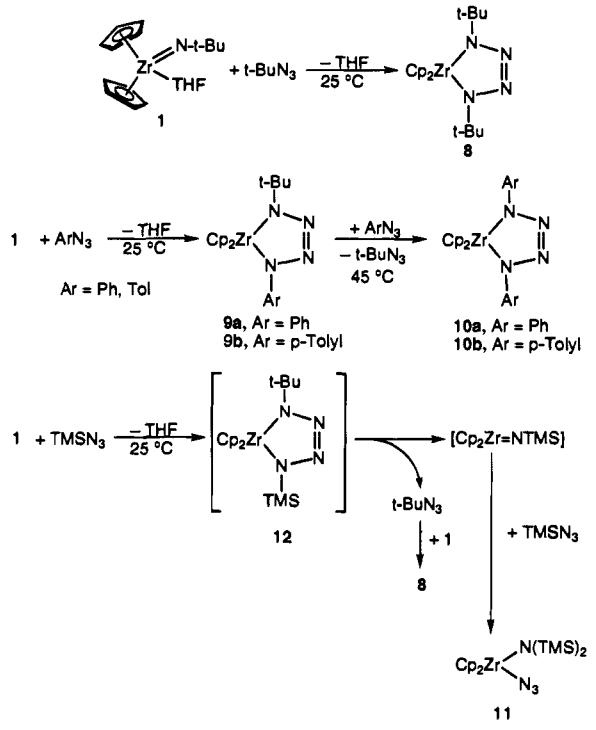

tetrazenes **9** underwent *loss* of organoazide (in this case, *t*-BuN_3). In the presence of ArN_3 **10a,b** were formed (90%); in the absence of free azide the reaction led to $[Cp_2ZrNAr]_2$. The formation of **9** and then **10** and *t*-BuN_3 (94%) was monitored by ^1H NMR spectroscopy in C_6D_6 and THF-d_8 solvents; clean conversion from **1** was observed at room temperature. The presence of *t*-BuN_3 in the volatile fraction of the reaction mixture was confirmed by comparison of its spectroscopic properties with those of an authentic sample.

A crystal of tetrazene **8** suitable for X-ray diffraction analysis was obtained by crystallization from toluene layered with pentane and cooled to −40 °C. The structure was solved by Patterson methods. The data collection parameters are contained in Tables 4 and 5 and the structure is shown in Figure 2. The bond distances and angles are found in Tables 6 and 7. The N1−N2 and N3−N4 distances are 1.38 Å, while the N2−N3 distance is 1.281 Å. The metal ring system is puckered with N2−N3 lying below the N1−Zr−N4 plane; the N1−Zr−N4 bond angle is 75.2°. Although the solid state structure of **2** is bent and therefore the Cp ligands are inequivalent, the complex

Scheme 4

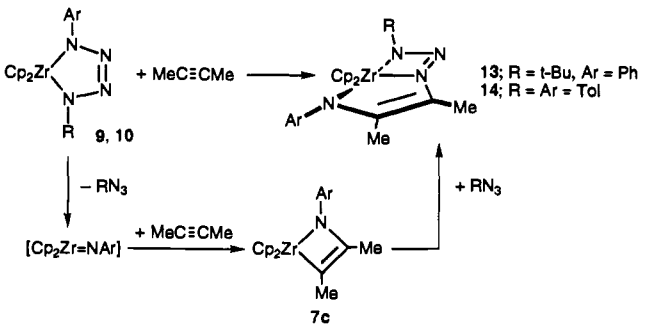

Scheme 5

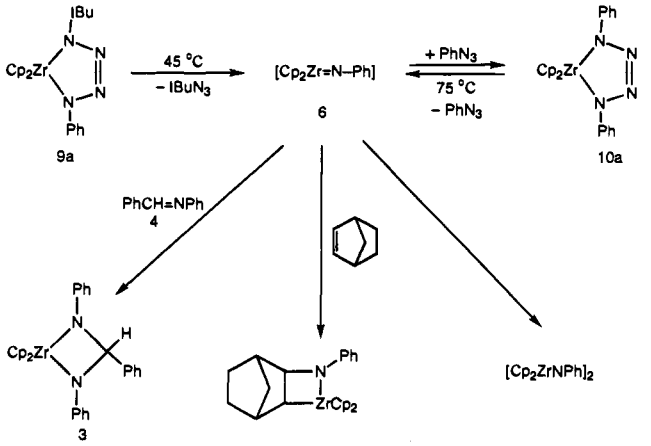

is fluxional in solution even at low temperatures as analyzed by ^1H NMR spectroscopy.

The reaction of imido complex **1** with Me_3SiN_3 did not lead to an isolable silyl-containing tetrazene complex. Instead, compound **8** was isolated in 34% yield with another complex that was identified as the zirconium azide $Cp_2Zr(N(SiMe_3)_2)(N_3)$ (**11**) in 35% yield (Scheme 3). The IR spectrum of the amide azide complex displays two intense bands at 2094 and 802 cm^{-1} typical for group IV metal azides. In addition, one of the largest peaks in the EI mass spectrum corresponds to the ion $[Cp_2Zr(N(SiMe_3)_2]^+$ obtained upon loss of N_3^-. Finally, the spectroscopic properties of **11** are similar to those of the crystallographically characterized compound, $Cp^*_2Ti(OSiMe_3)(N_3)$.[32] The reaction of **1** with Me_3SiN_3 was monitored by ^1H NMR spectroscopy; the formation of a metastable zirconium intermediate and release of *t*-BuN_3 were observed prior to formation of **8** and **11**. The intermediate is proposed to be the [3 + 2] cycloaddition product **12**.

When tetrazene complexes **9** and **10** were heated in the absence of a trapping reagent, the imido dimer $[Cp_2Zr(NAr)]_2$ was cleanly generated in 93−97% yield (NMR). While complex **9** undergoes this cycloreversion reaction at a moderate temperature (45 °C), complex **10** is stable to 75 °C. In an effort to trap the intermediate $[Cp_2Zr{=}NAr]$, **9** was thermolyzed in the presence of $Ph_3P{=}O$, and the reaction was monitored by ^1H NMR spectroscopy. Upon loss of *t*-BuN_3, a new Cp resonance appeared that was attributed to $Cp_2Zr(=NAr)(OPPh_3)$; however, this species was eventually converted to dimer. More successful trapping was obtained with strained alkenes and imines: as illustrated in Scheme 5, heating a benzene solution of **9** with bicyclo[2.2.1]hept-2-ene (norbornene) gave *t*-BuN_3 and the azametallacycle reported earlier[8] and reaction with

(32) This complex is formed in the reaction of $Cp^*_2Ti(=O)$(pyridine) with an equivalent of $TMSN_3$. Polse, J. L.; Andersen, R. A.; Bergman, R. G. unpublished results.

Table 4. Crystal Parameters for Complexes **8** and **14**

	8	**14**
empirical formula	$ZrN_4C_{18}H_{28}$	$ZrN_4C_{28}H_{30}$
formula wt (amu)	391.7	513.8
size	0.25 × 0.27 × 0.43	0.08 × 0.20 × 0.25 mm
space group	$P2_12_12_1$	$P2_1/n$
a	8.5618(13)	9.927(2) Å
b	14.4507(18)	13.377(2) Å
c	15.1037(17)	18.068(3) Å
α	90.0	90.0°
β	90.0	97.605(14)°
γ	90.0	90.0°
V (Å^3)	1868.7(7)	2378.3(13)
Z	4	4
d_{calc} (g cm^{-3})	1.39	1.43
μ_{calc} (cm^{-1})	5.8	4.8

Table 5. Data Collection Parameters for Complexes **8** and **14**

	8	**14**
temp (°C)	-112	-95
refl. measd	$\pm h,+k,+l$	$+h,+k,\pm l$
scan width	0.90 + 0.35tanθ	$\Delta\theta = 0.70 + 0.35 \tan\theta$
scan speed (θ deg/min)	8.24	5.49
vert aperture (mm)	4.0	4.0
horiz aperture (mm)	2.0 + 1.0 tanθ	2.0 + 1.0 tanθ
no. refl collected	2676	3213
no. unique refl	2652	2861
no. refl $F^2 > 3s(F^2)$	2491	1720
I_{min}/I_{max}	0.952	0.858
no. params	98	138
$R(F)$ (%)	4.8	7.2
$R_w(F)$ (%)	6.6	8.3
R_{all} (%)	5.1	13.6
goodness of fit	2.97	2.43
p-factor	0.03	0.03

PhN=CHPh generated the diazametallacycle Cp_2Zr(NPh-CHPhNAr) (**3**).

Reactions of the Tetraazacyclopentene Complex with Alkynes. In the presence of 2-butyne or diphenylacetylene, thermolysis of **9** or **10** yielded the novel insertion products **13** and **14** in 77% and 65% yields, respectively. While spectroscopic data were consistent with the structural assignment of the insertion product illustrated in Scheme 4, an X-ray diffraction study of **14a** was necessary for an accurate description of this unusual molecule. The structure was solved by Patterson methods. The data collection parameters and selected bond distances and angles are found in Tables 4–7, and an ORTEP representation is found in Figure 3. The product is formally a seven-membered metallacycle consisting of coplanar four- and five-membered ring systems. The bonding distances within the five-membered ring (N3–C25, 1.38(1) Å; C25–C26, 1.39(2) Å; C26–N4, 1.38(1) Å) indicate delocalization of the C–C double bond. The Zr–N3 distance of 2.19(1) Å is shorter than the Zr–N1 or Zr–N4 distances of 2.38(1) and 2.29(1) Å, respectively. Coordination of all three nitrogen atoms gives the zirconium center an 18-electron count.

The formation of the seven-membered metallacycle **13** was monitored by ^{1}H NMR spectroscopy. Scheme 4 illustrates the proposed reaction sequence. When **9** was heated to 45 °C in benzene-d_6, resonances corresponding to the tetrazene decreased in intensity, while peaks attributed to t-BuN_3 and a metallacyclobutene intermediate (**7c**) appeared. Following this, t-BuN_3 reacted with the metallacyclobutene complex, and resonances assigned to **13** grew in. The related metallacyclobutene Cp_2-Zr(N(2,6-$Me_2C_6H_3$)C(Me)=C(Ph)) (**15**) was prepared independently and treated with $TolN_3$ in benzene (eq 11). Insertion of the azide into the Zr–C bond generated the analogous seven-membered metallacycle **16** (eq 11) in >90% yield by NMR spectroscopy.

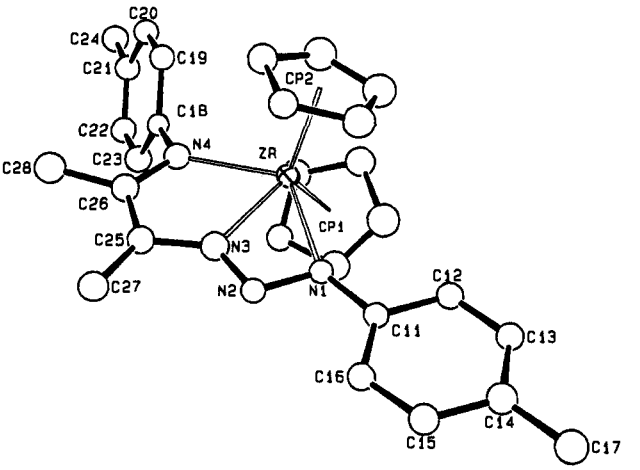

Figure 3. ORTEP diagram illustrating the geometry and labeling scheme for complex **14**. The spheres are scaled to represent the 50% probability surface.

Table 6. Selected Intramolecular Distances for **8** and **14**

atom 1	atom 2	distance
	Complex **8**	
Zr	N1	2.126(6)
Zr	N4	2.117(6)
Zr	Cp1	2.224
Zr	Cp2	2.247
N1	N2	1.386(8)
N1	C11	1.471(9)
N2	N3	1.281(8)
N3	N4	1.384(8)
N4	C15	1.503(9)
	Complex **14**	
Zr	N1	2.387(11)
Zr	N3	2.196(12)
Zr	N4	2.292(11)
Zr	Cp1	2.223
Zr	Cp2	2.235
N1	N2	1.348(14)
N1	C11	1.399(15)
N2	N3	1.286(14)
N3	C25	1.387(16)
N4	C18	1.412(16)
N4	C26	1.381(16)
C25	C26	1.389(18)
C25	C27	1.460(19)
C26	C28	1.528(18)

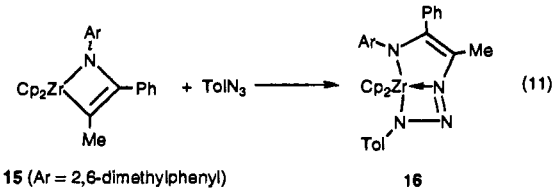

15 (Ar = 2,6-dimethylphenyl) **16**

Discussion

Zirconium Mediated Imine Metathesis. The imidozirconium complex **1** reacts with unsaturated organic compounds to yield [2 + 2] cycloaddition products. In the case of benzaldehyde N-phenylimine, the product is the diazametallacyclobutane complex **2**. Formation of metallacycle **2** from **1** is believed to occur by a dissociative pathway, in analogy to the mechanism

Table 7. Selected Intramolecular Angles for **8** and **14**

atom1	atom2	atom3	angle
		Complex **8**	
N1	Zr	N4	75.21(22)
N1	Zr	Cp1	112.21
N1	Zr	Cp2	108.86
N4	Zr	Cp1	112.03
N4	Zr	Cp2	108.50
Cp1	Zr	Cp2	127.77
Zr	N1	N2	106.6(4)
N1	N2	N3	118.1(6)
N2	N3	N4	118.3(6)
Zr	N4	N3	106.9(4)
		Complex **14**	
Cp1	Zr	Cp2	129.3
Cp1	Zr	N1	100.7
Cp2	Zr	N1	98.8
Cp1	Zr	N3	118.8
Cp2	Zr	N3	110.5
Cp2	Zr	N4	104.1
Cp2	Zr	N4	104.6
N1	Zr	N3	53.6(4)
N1	Zr	N4	121.3(4)
N3	Zr	N4	67.8(4)
Zr	N1	N2	95.5(7)
N1	N2	N3	103.9(11)
Zr	N3	N2	107.0(9)
Zr	N3	C25	126.4(9)
N2	N3	C25	126.0(12)
Zr	N4	C26	116.8(9)
N3	C25	C26	108.1(13)
N3	C25	C27	121.1(12)
N4	C26	C25	119.7(13)
N4	C26	C28	119.8(12)

proposed for the reaction of **1** with alkynes.[33] Initial reversible dissociation of the THF ligand generates the transient coordinatively unsaturated imido complex $Cp_2Zr{=}N\text{-}t\text{-}Bu$, and the rapid reaction of this intermediate with the unsaturated organic compound gives the metallacycle (eq 12).[25] That the formation of **2** occurs much more slowly in THF solvent is evidence for this proposal.

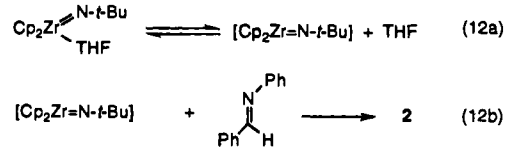

At elevated temperatures and in the presence of excess imine **4**, the metallacycle **2** undergoes a reaction that resembles olefin metathesis. The new symmetrical metallacycle **3** forms, and imine **5** is extruded. The thermolysis of **2** or **3** was found to generate the dimer $[Cp_2Zr(NPh)]_2$. We believe these transformations occur through the formation of a reactive imido complex $Cp_2Zr{=}NPh$ which is closely related to $Cp_2Zr{=}N\text{-}t\text{-}Bu$. Attempts to isolate the *N*-phenylimido species, however, have been unsuccessful.

We considered two reasonable mechanisms for the conversion of **2** to **3**. The first is an associative process that involves direct attack of *N*-phenylimine **4** on diazametallacycle **2**. This reaction should follow a rate law that is first order in **2** and first order in **4** (rate = k'[**2**][**4**]). An alternative dissociative mechanism is outlined in Scheme 2. In a pre-equilibrium step *N*-*tert*-butylimine **5** is released, and the transient imido complex **6** is formed. Subsequent reaction of the intermediate **6** with *N*-phenylimine **4** generates the new diazametallacycle **3**. Experiments with both **3** and **5** showed that although the reaction is reversible (see below), if only modest concentrations of **5** are utilized in the kinetic study the back reaction remains slow enough that the k_{-2} step can be ignored. Utilizing this assumption and applying the steady state approximation to the concentration of **6** predicts the rate law shown in eq 8a. If this mechanism controls the reaction, only under the conditions of k_{-1}[**5**] $\gg k_2$[**4**] will the rate law give first order behavior in [**2**] and [**4**], and under these conditions the rate should show inhibition by added *N*-*tert*-butylimine **5**. As k_2[**4**] becomes much greater than k_{-1}[**5**], the reaction will reach saturation. At this concentration of **4** the reaction order in both imines **4** and **5** should go to zero, and the observed rate will level off at k_1[**2**], as predicted by eq 8a.

As noted in the Result section, the experimental kinetic results agree with the proposal of a dissociative mechanism. From the inverse plot (eq 8b, inset Figure 1), we obtained values for $k_1 = 1.4 \pm 0.1 \times 10^{-3}$ s^{-1} and $k_{-1}/k_2 = 0.34 \pm 0.02$. The k_{-1}/k_2 ratio demonstrates that the transient imido complex is trapped more rapidly by *N*-phenylimine than by *N*-*tert*-butylimine. Under conditions that favor the k_{-2} back reaction, we were able to measure an equilibrium constant $K_{eq} = 4.6$ for the reaction. Thus, the higher thermodynamic stability of [**3** + **5**] over [**2** + **4**] is reflected to some extent in the transition states leading to the two metallacycles.

If the dissociative mechanism is correct, it should be possible to trap transient imido complex **6** generated from metallacycle **2** with alkynes. Furthermore, these reactions should also demonstrate saturation kinetics, and the saturation rate constant k_1 should be identical to that measured in the imine metathesis study. We therefore examined the addition of diphenylacetylene and 2-butyne to diazametallacycle **2**. As illustrated in Scheme 2, the phenylimido intermediate **6** identified as the first intermediate generated in the imine metathesis reaction can now be trapped by alkyne rather than by a second molecule of imine. This gives the rate law shown in eq 13.

$$\text{rate} = \frac{k_1 k_3[\mathbf{2}][\text{alkyne}]}{k_{-1}[\mathbf{5}] + k_3[\text{alkyne}]} \qquad (13a)$$

$$k_3[\text{alkyne}] \gg k_{-1}[\mathbf{5}]; \quad \text{rate} = k_1[\mathbf{2}] \qquad (13b)$$

A series of kinetic studies similar to those mentioned above demonstrated that the reaction was first order in [**2**] but zero order in [alkyne] even at the lowest concentrations of this reactant that we were conveniently able to reach while still maintaining pseudo-first order conditions in [**2**]. Therefore, the reaction clearly does not involve initial attack of alkyne on the diazametallacycle. If the dissociative mechanism is presumed to occur, then under all of our conditions k_3[alkyne] $\gg k_{-1}$[**5**] (i.e., the alkynes trap imido complex **6** more rapidly than does *N*-phenylimine **4**) and the rate simplifies to k_1[**2**] (eq 13b). Important support for this assumption is provided by the fact that the k_1 values determined from these rate studies are the same for both alkynes and identical within experimental error to the k_1 value measured in the imine metathesis kinetic experiments.

As expected from the reversibility studies mentioned above, heating **3** with diphenylacetylene also leads to **7a**, but more slowly than this complex is formed from **2**. Under the conditions of excess diphenylacetylene, $k_{obs} = k_{-2} = 0.90 \pm 0.05 \times 10^{-3}$ s^{-1}. The conditions of the reaction were also varied in order to examine the equilibrium between **2** and **7a**. A value of $K_{eq} = 7.4$ was determined for this reaction at 70 °C. This

(33) Kinetic studies on the closely related reaction of $Cp_2Zr(N\text{-}t\text{-}Bu)(OPPh_3)$ with alkynes support this mechanism: Lee, S. Y.; Bergman, R. G., unpublished results.

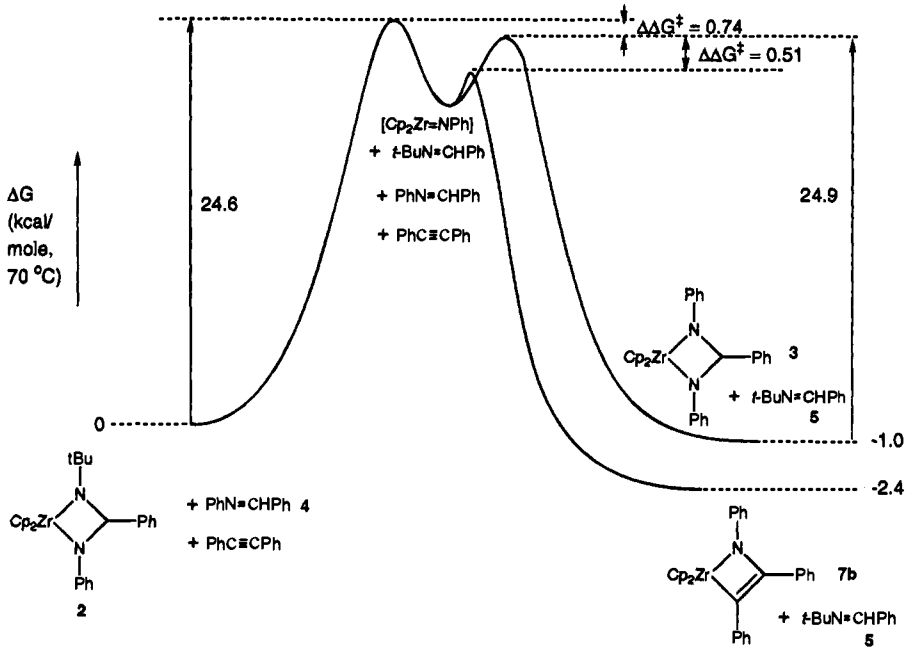

Figure 4. Reaction coordinate/free energy diagram for the interconversion of diaza- and azametallacycles **2**, **3**, and **5**.

demonstrates the stability of [**7a** + **5**] over [**2** + alkyne]. Finally, competition experiments were utilized to determine the relative abilities of **4**, 2-butyne, and diphenylacetylene to trap the reactive imido species **6**. Reactions of **2** with competing amounts of two reagents were monitored at early reaction times, and the product ratios were measured. In this manner we were able to calculate values for $k_3/k_2 = 2.1$ and $k'_3/k_3 = 1.4$. A summary of the rate constants and ratios determined for this system is given in Scheme 2.

The information obtained in these kinetic studies was used to generate the free energy diagram illustrated in Figure 4. Starting at the left side, complex **2** (set arbitrarily at $\Delta G°$(70 °C) = 0 kcal/mol) undergoes cycloreversion to generate the reactive phenylimido intermediate **6**. The free energy of activation for this process $\Delta G^{\ddagger}$(70 °C) = 24.6 kcal/mol. Intermediate **6** can be trapped by either imine **4** or diphenylacetylene, or it can react with imine **5** and regenerate **2**. The free energies of the three transition states involved in these transformations differ by the amounts derived from the competition experiments. The state that leads to diazametallacycle **3** lies 0.74 kcal/mol lower in energy than the transition state for reconversion to **2** and 0.50 kcal/mol higher in energy than the state that leads to metallacyclobutene **7a**. The overall reactions to give the two products **3** and **7a** are exoergic by −1.0 and −2.4 kcal/mol, respectively.

Organoazide Cycloadditions and -reversions. The imidozirconium complex **1** undergoes [2 + 3] cycloaddition reactions with organoazides to generate tetraazametallacyclopentene (tetrazene) complexes **8** and **9**.[34,35] Examples of electron deficient early transition-metal tetrazene complexes are rare.[22] Structural characterization of analogous mid and late transition-metal tetraazacyclopentene complexes have shown metal-ligand ring systems that are essentially planar. However, as shown in Figure 2 the zirconium complex contains a puckered ring with the nitrogen atoms in the 2,3-position below the plane. This structural feature resembles the bending observed in group IV diazametallacyclopentenes where the C=C portion of the ring also lies beneath the plane.[31,36–38] The N2–N3 distance of 1.28 Å is 0.1 Å shorter than the other N–N distances, indicating that the double bond is localized between N2 and N3.

Scheme 6

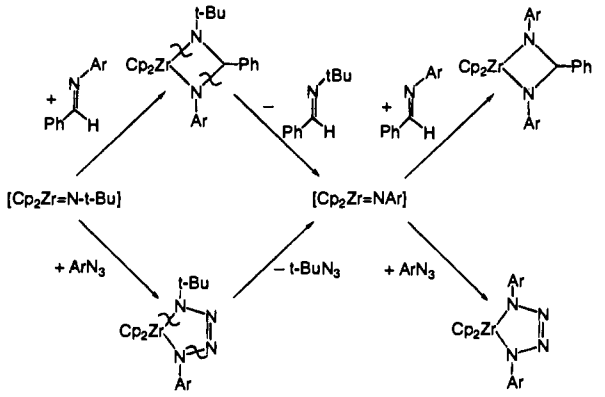

The reaction of **1** with 2 equiv of Me_3SiN_3 does not generate an isolable tetrazene complex with Me_3Si- groups in the 1- and 4-positions. Instead, two complexes were formed in the reaction that were identified as tetrazene complex **8** and $Cp_2Zr(N(SiMe_3))(N_3)$ (**11**). Formation of amide azide **11** is also believed to occur via the reaction pathway outlined in Scheme 3. Transfer of a Me_3Si- group from trimethylsilylazide has also been observed in reactions with $Me_2Si(t\text{-BuN})_2Ge$ to generate $Me_2Si(t\text{-BuN})_2Ge(N(SiMe_3)_2)(N_3)$.[25] It is interesting to note the similarity between our zirconium system and the chemistry of Neumann's germanium compounds.

Zirconium-Mediated Azide Metathesis. The reactivity of complex **9** shows an interesting similarity to that of metallacyclobutane complex **2**. Once formed, addition of another equivalent of organoazide to **9** at 45 °C leads to an "azide metathesis" reaction. The symmetrical tetrazene complex **10** is formed and $t\text{-BuN}_3$ is generated.

(34) Rosen, R. Ph.D. Thesis, University of California, Berkeley, 1990.
(35) Pritzkow, V. W.; Timm, D. *J. Prakt. Chem.* **1966**, *4*, 178.
(36) Bocarsly, J. R.; Floriani, C.; Chiesi-Villa, A.; Guastini, C. *Organometallics* **1986**, *5*, 2380.
(37) Berg, F. J.; Petersen, J. L. *Organometallics* **1991**, *10*, 1599.
(38) Bol, J. E.; Hessen, B.; Teuben, J. H.; Smeets, W. J. J.; Spek, A. L. *Organometallics* **1992**, *11*, 1981.

As illustrated in Scheme 6, we believe that a dissociative mechanism is also involved in the conversion of **9** to **10**. As before, the first step involves reversible loss of t-BuN_3 to generate the reactive imido complex $Cp_2Zr{=}NAr$ (Ar = Ph, Tol) and attack of the reactive imido species by the incoming arylazide gives the new tetrazene complex. To support this proposal, we attempted to trap the imido intermediate presumed to be formed in these reactions. Heating **9** to 45 °C in the absence of added trapping reagents generated the dimer $[Cp_2Zr(NAr)]_2$. Similarly, at 75 °C, thermolysis of **10** also gave the dimer product. The notable difference between the temperatures neccessary for **9** and **10** to undergo cycloreversion gives an indication of the greater stability of the symetrically substituted tetrazene complex. It is likely that that loss of t-BuN_3 is favored due to polarization of the tetrazene ring system in the unsymmetric complex (symmetric tetrazene complex **8** also requires higher temperatures for cycloreversion to occur). When thermolysis of **9b** was carried out in the presence of Ph_3PO, we observed an intermediate by ^1H NMR spectroscopy that we believe is $Cp_2Zr(=NTol)(OPPh_3)$; however, this complex reacted quickly to give the thermodynamically favored dimer. Norbornene reacted with the intermediate imido complex to form the azametallacyclobutane product characterized earlier[8] in the reaction of **1** with this alkene (Scheme 5), but dimer formation was still a substantial side reaction. In the presence of imine **4**, the imido complex was successfully trapped to give the diazametallacyclobutane product **3**.

Our attempt to use an alkyne to trap the imido intermediate proved to be more complicated. Upon addition of 2-butyne to either metallacycle **9** or **10** at 45 °C or 135 °C, respectively, an azide insertion product (**13** or **14**), rather than the expected azametallacyclobutene complex was formed. An analogous reaction occurs when **9** or **10** is treated with diphenylacetylene. The reaction was determined to proceed in a stepwise fashion by detection of the NMR-observable release of t-BuN_3 (Scheme 4) and the formation of azametallacyclobutene complex **7c**. In a second step, insertion of the released organoazide into the Zr−C bond of the metallacyclobutene leads to the product. This reaction pathway was confirmed through an independent synthesis of a similar metallacyclobutene complex (**15**, eq 11) and reaction with tolylazide to give the analogous reaction product **16**. A related insertion of an organic azide into the metal−carbon bond of an oxazirconacyclobutene with Cp* (i.e., η^5-C_5Me_5) ligands has been observed by Hillhouse. The terminal nitrogen, which coordinates to zirconium in **13a**, remains uncoordinated in Hillhouse's molecule, presumably due to steric repulsions between the large Cp* ligands and the potentially coordinating azide N−R group.[39]

Conclusion

In summary, reactive imidozirconium complexes have been shown to undergo overall [2 + 2] and [3 + 2] cycloaddition reactions. This report has focused on the addition of organic imines and azides to the Zr=NR moiety to generate diazazirconacyclobutane and tetraazazirconacyclopentene complexes, respectively. The two reaction systems show some interesting similarities (Scheme 6). Initial addition of the organic substrate occurs quickly at room temperature; at higher temperatures cycloreversion reactions take place. When the latter reaction is carried out in the presence of imine or azide reagent, the arylimido intermediate is trapped as the symmetrical metallacycle, or it can be trapped by other unsaturated organic reagents. There is a notable difference in the temperatures required for the cycloreversion steps. The unsymmetrical tetrazene is the least stable metallacycle and eliminates t-BuN_3 at 45 °C, while the other complexes require longer reaction times at temperatures above 70 °C. We expect that further studies will confirm that reversible cycloadditions are quite general transformations for this class of complexes.

Experimental Section

General Methods. Unless otherwise noted, all manipulations were carried out under an inert atmosphere in a Vacuum Atmospheres 553-2 drybox with attached MO-40-2 Dritrain or by using standard Schlenk or vacuum line techniques. Solutions were degassed by sequentially freezing to −196 °C, evacuating under high vacuum and thawing. This sequence was used three times in each case. Glass reaction vessels fitted with ground glass joints and Kontes Teflon stopcocks are referred to as bombs.

^1H and $^{13}C\{^1H\}$ NMR spectra were obtained on either a 300 or 400 MHz Bruker AMX series Fourier transform spectrometer, and the carbon data were obtained at 75.4 or 100.6 MHz, respectively. Sealed NMR tubes were prepared using Wilmad 505-PP and 504-PP tubes attached by Cajon adapters directly to Kontes vacuum stopcocks and degassed with freeze−pump−thaw cycles before flame sealing.

IR spectra were obtained on a Mattson Galaxy Series FTIR 3000 spectrometer. Elemental analyses were obtained from the UCB Microanalytical Laboratory. Mass spectroscopic (MS) analysis were obtained at the UCB mass spectrometry facility on AEI MS-12 and Kratos MS-50 mass spectrometers.

Unless otherwise specified, all reagents were purchased from commercial suppliers and used without further purification. Pentane and hexanes (UV grade, alkene free) were distilled from sodium benzophenone ketyl/tetraglyme under nitrogen. Benzene, toluene, diethyl ether, and THF were distilled from sodium benzophenone ketyl under nitrogen. Deuterated solvents for use in NMR experiments were dried as their protiated analogs but were vacuum transferred from the drying agent. The imine reagents were synthesized in condensation reactions from the parent amine and aldehyde and were dried as benzene solutions over activated 4 Å molecular sieves. $Cp_2Zr(N$-t-$Bu)(THF)$,[40] PhN_3 and $TolN_3$,[34,41] and t-BuN_3[35] were prepared by literature methods.

$Cp_2Zr(N(t$-$Bu)CH(Ph)N(Ph))$ (2). The imido complex **1** (0.103 g; 0.0282 mmol) was dissolved in 3 mL of toluene, and imine **4** (0.0563 g, 0.0311 mmol) was added. The solution was shaken until homogeneous at which point the color had changed from yellow to red. Upon allowing the reaction mixture to stand, red crystals formed after several hours and were collected by decanting the solvent and washing with 5 mL of hexanes: yield 0.122 g (91%); IR (Nujol) 1488, 1355, 1432, 1228, 1210, 1189, 1177, 1088, 1063, 1040, 1027, 1010, 990, 823, 792, 772, 743, 703, 689, 677, 657 cm^{-1}; ^1H NMR (300 MHz, CD_2Cl_2) δ 0.83 (s, 9H, $C(CH_3)_3$), 4.90 (s, 1H, C-*H*), 6.16 (dd, J_{HH} = 1.03, 8.08 Hz, 2H, C-*H*), 6.22 (s, 5H, C_5H_5), 6.41 (tt, J_{HH} = 1.07, 7.25 Hz, 1H, C-*H*), 6.53 (s, 5H, C_5H_5), 6.92 (t, J_{HH} = 7.26 Hz, 2H, C-*H*), 7.11 (t, J_{HH} = 7.30 Hz, 1H, C-*H*), 7.22 (t, J_{HH} = 7.45 Hz, 2H, C-*H*), 7.45 (dd, J_{HH} = 1.31, 7.63 Hz, 2H, C-*H*); $^{13}C\{^1H\}$ NMR (CD_2Cl_2) δ 34.41 ($C(CH_3)_3$), 55.19 ($C(CH_3)_3$), 62.40 (*C*HPh), 110.40 (*C*-H), 112.77 (C_5H_5), 113.54 (C_5H_5), 114.79 (*C*-H), 119.07 (*C*-H), 126.43 (*C*-H), 126.67 (*C*-H), 127.39 (*C*-H), 127.62 (*C*-H), 128.17 (*C*-H), 128.33 (*C*-H), 130.45 (*C*-H), 144.13 (quat), 151.96 (quat); λ_{max} = 506 nm (ϵ = 354). Anal. Calcd for $C_{27}H_{30}N_2Zr$: C, 68.45, H, 6.38, N, 5.91. Found: C, 68.17; H, 6.45; N, 5.82.

$Cp_2Zr(N(Ph)CH(Ph)N(Ph))$ (3). A glass bomb was charged with the monomeric imido complex **1** (0.0927 g, 0.0254 mmol), PhNCHPh (**4**) (0.138 g, 0.0762 mmol), and 8 mL of benzene. As the solvent was added the solution instantly turned red with the formation of **2**. The solution was degassed and heated to 85 °C for 1 h during which time the solution turned purple. Upon standing, purple crystals formed on the walls of the reaction vessel and were isolated by decanting the solution and washing with 3 mL of benzene: yield 0.117 g (93%); IR

(39) Vaughan, G. A.; Hillhouse, G. L.; Rheingold, A. L. *J. Am. Chem. Soc.* **1990**, *112*, 7994. We are grateful for a helpful comment on this point by a thoughtful referee.

(40) Walsh, P. J.; Baranger, A. M.; Bergman, R. G. *J. Am. Chem. Soc.* **1992**, *114*, 1708.

(41) Smith, P. A. S. *Org. Syn.* **1951**, *31*, 14.

(Nujol) 1563, 1488, 1348, 1330, 1305, 1280, 1265, 1088, 1014, 953 (s), 812, 801, 752, 743, 715 (s), 690, 679, 655, 641 cm^{-1}; ^1H NMR (300 MHz, CD_2Cl_2) δ 5.26 (s, 1H, C-*H*), 6.24 (s, 5H, C_5H_5), 6.75 (dd, J_{HH} = 0.96, 8.56 Hz, 4H, C-*H*), 6.51 (tt, J_{HH} = 7.20, 1.01 Hz, 2H, C-*H*), 6.75 (s, 5H, C_5H_5), 7.01 (t, J_{HH} = 7.85 Hz, 4H, C-*H*), 7.13 (tt, J_{HH} = 1.55, 8.59 Hz, 1H, C-*H*), 7.27 (t, J_{HH} = 7.92 Hz, 2H, C-*H*); $^{13}C\{^1H\}$ NMR (CD_2Cl_2) δ 64.39 (*C*HPh), 115.21 (C_5H_5), 115.61 (C_5H_5), 115.72 (*C*-H), 116.91 (*C*-H), 127.36 (*C*-H), 128.35 (*C*-H), 129.07 (*C*-H), 129.15 (*C*-H), 142.11 (quat), 152.67 (quat). λ_{max} = 558 nm (ϵ = 220). Repeated attempts to obtain a successful microanalysis on this complex failed. The loss of *tert*-butylimine **5** in the reaction was confirmed by ^1H NMR spectroscopy and comparison with an authentic sample of the imine.

Kinetic Studies of the Imine Metathesis Reaction. Both ^1H NMR and UV−vis spectrometry were used to study the stoichiometric imine metathesis reaction that converts complex **2** to **3**. In the ^1H NMR experiments, cyclohexane was used as the internal standard. The disappearance of **2** and formation of **3** were monitored as the reaction progressed at 70 °C. The instruments were temperature calibrated prior to their use by standard techniques.

For the UV−vis experiment, stock solutions of **2** were prepared before each series of kinetic experiments. Decomposition of these solutions to dimer prevented their storage for long periods of time; between each kinetic experiment the solutions were stored in the drybox at −40 °C. A typical stock solution (no. 1) of **2** contained 0.0525 g (0.111 mmol) of the complex dissolved in 10.00 mL of toluene in a volumetric flask. Stock solution no. 2 contained 0.2451 g (1.520 mmol) of imine **5** also dissolved in 10.00 mL of toluene in a volumetric flask. These solutions were also stored at −40 °C in the drybox.

In a typical experiment a 2.00 ± 0.01 mL volumetric flask was charged with 0.60 mL of stock solution no. 1, 0.30 mL of solution no. 2, and 0.0745 g (0.411 mmol) of imine **4**. Toluene solvent was added to bring the total volume to 2.00 mL. The solution was transferred to a gas tight UV−vis cell with a Kontes Teflon stopcock seal and equipped with a stir bar. The sample was then placed in UV−vis spectrometer, and the data were collected at 1-min intervals. The absorbance intensities of starting material **2** and product **3** at λ_{max} = 506 and 558 nm, respectively, were monitored and plotted versus time. The data were then analyzed with an exponential fitting program.

The stock solutions used in the NMR experiments were prepared in the same manner, but the concentrations were greater and toluene-d_8 was used as the solvent and cyclohexane was added as an internal standard. The samples were prepared as before, transferred to an NMR tube, degassed by two freeze−pump−thaw cycles, and then flame sealed. A 300 MHz Bruker NMR instrument was used in the data collection, and a program was used to aquire the one-pulse ^1H NMR spectrum at 2-min intervals. The integrals of the complexes **2** and **3** were determined. A sample solution was prepared, and the imine metathesis reaction was monitored by ^1H NMR and UV−vis spectrometry. The data obtained from these experiments compared favorably (Table 1).

Kinetic Studies of the Reaction of 2 with Alkynes. Similar procedures were used to monitor the formation of metallacyclobutene **7** in the trapping reactions of **2** with diphenylacetylene or 2-butyne. The kinetic samples were prepared as before with stock solutions no. 1 and no. 2 and weighed amounts of the alkyne reagents. The reactions were monitored using the methods previously described, and the data were analyzed with and exponential fitting program. Rate constants are listed in Tables 2 and 3.

Equilibrium and Competition Experiments. A series of NMR samples were prepared as described above that contained known weights of complexes **2** or **3** and mixtures of phenylimine **4** and *tert*-butylimine **5** or phenylimine **4** and diphenylacetylene dissolved in 0.5 mL of toluene solvent. These reactions were monitored by ^1H NMR spectroscopy. For the equilibrium experiments, data were collected at the beginning of the reaction, and then the NMR tube was placed in a constant temperature bath at 70 °C for 24 h. A final ^1H NMR spectrum was obtained and this was used to calculate K_{eq}. In the competition experiments, the reactions were heated in the probe of the NMR instrument. The data were collected at 2-min intervals; and the product integral ratios were measured at early reaction times.

Catalytic Imine Metathesis Reaction. A solution was prepared containing 0.028 g (0.015 mmol) of imine **4** and 0.028 g anisaldehyde *N*-*p*-tolylimine in 1.0 mL toluene-d_8. An NMR tube was charged with 0.30 mL of this solution, 0.0058 g (0.012 mmol) of **2**, and sufficient toluene-d_8 to bring the total volume to 0.5 mL. The tube was degassed and flame sealed, and the ^1H NMR spectrum of this mixture was obtained. The reaction was then placed in a 70 °C constant temperature bath for 12 h. After this time, the ^1H NMR spectrum was measured and found to display resonances due to a statistical mixture of the four possible imine products from the imine metathesis reaction. Similar results were obtained when complex **3** (0.0044 g; 0.0089 mmol) was utilized in the reaction. At lower concentrations of zirconium complex, complete scrambling of the imines was hindered by dimer formation.

$Cp_2Zr(N(t\text{-}Bu)N{=}NN(t\text{-}Bu))$ (8). In the drybox imido complex **1** (0.0235 g, 0.0644 mmol) was dissolved in 5 mL of benzene. A 1-mL benzene solution that contained 1 equiv of *t*-BuN_3 was slowly added to the solution of **1** at room temperature. The yellow solution turned purple as the reaction occurred. After 10 min, benzene was removed by evaporation under vacuum. The purple solid was recrystallized from a toluene solution layered with pentane and cooled to −40 °C: yield 0.0224 g (89%); IR (C_6D_6) 2972, 2935, 2362, 2295, 1365, 1024, 783 cm^{-1}; ^1H NMR (400 MHz, C_6D_6) δ 1.25 (s, 18H, $C(CH_3)_3$), 5.85 (s, 10H, C_5H_5); $^{13}C\{^1H\}$ NMR (400 MHz, C_6D_6, 298K) δ 31.1 ($C(CH_3)_3$), 60.3 ($C(CH_3)_3$), 109.3 (C_5H_5). Anal. Calcd for $C_{18}H_{28}N_4Zr$: C, 55.20, H, 7.21, N, 14.30. Found: C, 55.71; H, 7.75; N, 12.28.

$Cp_2Zr(N(SiMe_3)_2(N_3)$ (11). A solution of 0.0402 g (0.110 mmol) of **1** dissolved in 5 mL of benzene was prepared. To this was added another 1 mL benzene solution that contained 2 equiv of Me_3SiN_3 (0.0251 g, 0.218 mmol). The reaction mixture was stirred for 12 h during which time the yellow solution darkened to purple. Benzene was removed under reduced pressure, and a purple residue was obtained that by NMR spectroscopy was shown to contain two products. Upon extraction two times with 2 mL of pentane solvent, the insoluble purple tetraazene complex **8** was isolated cleanly (yield 0.0144 g, 34%). It was recrystallized and characterized as described in A. The pentane extracts were combined and evaporated to dryness. This fraction was found by NMR spectroscopy to contain mostly the colorless amide azide and traces of **2**: yield 0.0164 g (35%); IR (C_6H_6): 2094, 1599, 1360, 1254, 1201, 1034, 901, 812 cm^{-1}; ^1H NMR (300 MHz, C_6D_6) δ 0.12 (s, 9H, $Si(CH_3)_3$), 0.29 (s, 9H, $Si(CH_3)_3$), 5.85 (s, 10H, C_5H_5); $^{13}C\{^1H\}$ NMR (400 MHz, C_6D_6) δ 14.2 ($Si(CH_3)_3$), 15.8 ($Si(CH_3)_3$), 114.0 (C_5H_5); HRMS (EI) *m/e* calcd for $C_{16}H_{28}N_4Si_2Zr$ 422.0900, *m/e* found 422.0917.

Crystal Structure Determination for 8. Purple blocklike crystals of **8** were obtained by slow cooling of a toluene solution layered with pentane to −40 °C. One of these crystals was mounted on a glass fiber using Paratone N hydrocarbon oil. The crystal was then transferred to an Enraf-Nonius CAD-4 diffractometer and centered in the beam. It was cooled to −112 °C by a nitrogen flow low-temperature apparatus which had been previously calibrated by a thermocouple placed at the sample position. The cell parameters and specific data collection parameters for this data set are given in Tables 4 and 5. The 2676 raw intensity data were converted to structure factor amplitudes and their esd's by correction for scan speed, background, and Lorentz and polarization effects. Inspection of the intensity standards revealed that no correction for crystal decay was necessary. Space group $P2_12_12_1$ was confirmed by refinement. The structure was solved by Patterson methods and refined via standard least-squares and Fourier techniques. Inspection of the azimuthal scan data showed a variation of I_{min}/I_{max} = 0.952. An empirical absorption correction based on the differences of F_{obs} and F_{calc} after refinement of all atoms with isotropic thermal parameters was applied to the data. The final residuals for 98 variables refined against the 2491 data set for which $F^2 > 3\sigma(F^2)$ were R = 4.8%, wR = 6.6%, and GOF = 2.97. The R value for all 2652 data was 5.1%. The largest peak in the final difference Fourier map had an electron density of 1.21 e^-/A^3 and the lowest excursion −1.46 e^-/A^3. The quantity minimized by the least squares program was $\sum[w(|F_o| - |F_c|)^2]$, where w is the weight of a given observation. The p-factor, used to reduce the weight of intense reflections, was set to 0.03 in the last cycles of refinement. The analytical forms of the scattering factor tables for the neutral atoms were used, and all scattering factors were corrected for both the real and imaginary components of anomalous

dispersion. Positional parameters with isotropic thermal parameters and anisotropic thermal parameters are provided as supplementary information.

$Cp_2Zr(N(t\text{-}Bu)N{=}NN(Ph))$ (9a). To a 5-mL benzene solution that contained 0.0348 g of **1** (0.0954 mmol) was added 0.0112 g of PhN_3 (0.0940 mmol) in 1 mL of benzene. The reaction mixture immediately turned purple, and after 5 min the solvent was removed by evaporation under vacuum. The product was recrystallized from a toluene solution layered with pentane and cooled to −40 °C: yield 0.0383 g (98%) (purple solid); IR (C_6D_6) 2958, 2931, 2865, 1603, 1489, 1443, 1357, 1273, 1197, 1083, 951, 904, 800, 704, 781 cm^{-1}; ^1H NMR (400 MHz, C_6D_6) δ 1.14 (s, 9H, $C(CH_3)_3$), 5.85 (s, 10H, C_5H_5), 6.91 (d, J_{HH} = 7.4 Hz, 2H, C-*H*), 6.95 (t, J_{HH} = 7.4 Hz, 1H, C-*H*), 7.21 (t, J_{HH} = 7.4 Hz, 2H, C-*H*); $^{13}C\{^1H\}$ NMR (400 MHz, C_6D_6) δ 31.0 ($C(CH_3)_3$), 59.9 ($C(CH_3)_3$), 111.9 (C_5H_5), 119.4 (*C*-H), 122.7 (*C*-H), 128.6 (*C*-H), 128.7 (*C*-H). Anal. Calcd for $C_{20}H_{24}N_4Zr$: C, 58.35, H, 5.88, N, 13.61. Found: C, 57.93; H, 5.76; N, 13.16.

$Cp_2Zr(N(t\text{-}Bu)N{=}NN(Tol))$ (9b). In a procedure similar to that described above, a benzene solution of **1** (0.0230 g, 0.0631 mmol) was treated with $TolN_3$ (0.0087 g; 0.0653 mmol) in 1 mL of benzene to give the purple product. After 5 min the solution was evaporated to dryness under vacuum. The product was recrystallized from toluene layered with pentane and cooled to −40 °C: yield 0.0259 g (96%); IR (C_6D_6) 3091, 3047, 2956, 2873, 2368, 2123, 2087, 1817, 1508, 1491, 1282, 1211, 1038, 795, 677 cm^{-1}; ^1H NMR (400 MHz, C_6D_6) δ 1.20 (s, 9H, $C(CH_3)_3$), 2.22 (s, 3H, CH_3), 5.91 (s, 10H, C_5H_5), 6.85 (d, J_{HH} = 8.4 Hz, 2H, C-*H*), 7.02 (d, J_{HH} = 8.4 Hz, 2H, C-*H*); $^{13}C\{^1H\}$ NMR (400 MHz, C_6D_6) δ 20.6 (CH_3), 30.7 ($C(CH_3)_3$), 59.6 ($C(CH_3)_3$), 111.2 (C_5H_5), 119.3 (*C*-H), 128.3 (*C*-H), 129.0 (*C*-H), 131.6 (*C*-H). Repeated attempts to obtain satisfactory microanalysis and HRMS analysis data on this material were unsuccessful.

$Cp_2Zr(N(Ph)N{=}NN(Ph))$ (10a). The imido complex **1** (0.0240 g, 0.0658 mmol) was dissolved in 5 mL of benzene, and a separate solution was prepared with 2 equiv of PhN_3 (0.0163 g, 0.137 mmol) in 1 mL of benzene. These mixtures were combined and then heated to 45 °C for 30 min. After this time, the green solution was evaporated to dryness under vacuum to yield the product. Green crystals were obtained by recrystallization from toluene layered with pentane and cooled to −40 °C: yield 0.0269 g (95%); IR (C_6H_6) 1612, 1282, 1051, 933, 819, 727 cm^{-1}; ^1H NMR (400 MHz, C_6D_6, 298 K) δ 5.90 (s, 10H, C_5H_5), 6.79 (d, J_{HH} = 7.4 Hz, 4H, C-*H*), 6.95 (t, J_{HH} = 7.4 Hz, 2H, C-*H*), 7.19 (t, J_{HH} = 7.4 Hz, 4H, C-*H*); $^{13}C\{^1H\}$ NMR (400 MHz, C_6D_6,) δ 112.9 (C_5H_5), 118.1 (*C*-H), 122.7 (*C*-H), 128.3 (*C*-H), 129.6 (*C*-H). Repeated attempts to obtain satisfactory microanalysis and HRMS analysis data on this material were unsuccessful.

$Cp_2Zr(N(Tol)N{=}NN(Tol))$ (10b). As described above, a benzene solution of 0.0935 g (0.256 mmol) of **1** was treated with 2 equiv of $TolN_3$ (0.0701 g; 0.526 mmol) in benzene at 45 °C. The solution color turned green, and after 30 min the solution was evaporated to dryness under vacuum. The product was recrystallized from toluene layered with pentane at −40 °C yield 0.107 g (91%); IR (C_6D_6) 2935, 2879, 2104, 1605, 1512, 1273, 1097, 1024, 941, 802 cm^{-1}; ^1H NMR (400 MHz, C_6D_6) δ 2.23 (s, 6H, CH_3), 5.90 (s, 10H, C_5H_5), 6.80 (d, J_{HH} = 8.3 Hz, 4H, C-*H*), 7.03 (d, J_{HH} = 8.3 Hz, 4H, C-*H*); $^{13}C\{^1H\}$ NMR (MHz, C_6D_6, 298K) δ 20.6 (CH_3), 112.5 (C_5H_5), 118.3 (*C*-H), 128.3 (*C*-H), 129.2 (*C*-H), 131.9 (*C*-H). Anal. Calcd for $C_{24}H_{24}N_4Zr$: C, 62.71, H, 5.26, N, 12.19. Found: C, 62.67; H, 5.27; N, 12.21.

Formation of $t\text{-}BuN_3$. The reaction of **1** with $TolN_3$ was carried out as described above for the preparation of **9a**. Upon completion, the green solution was transferred to a reaction bomb, removed from the drybox, and placed on a vacuum line where it was degassed. The volatile material from the reaction mixture (C_6H_6 and $t\text{-}BuN_3$) was transferred under vacuum to another bomb cooled to −196 °C. The ^1H NMR and IR spectroscopic properties of this mixture were compared to an authentic sample of $t\text{-}BuN_3$. A yield of 94 −100% $t\text{-}BuN_3$ formation was determined from sealed NMR tube reactions. IR (C_6H_{12}) 2102 cm^{-1}; ^1H NMR (400 MHz, C_6D_6) δ 0.92 (s, 9H).

Reaction of 9 with Norbornene. A solution that contained 0.0022 g (0.0054 mmol) of **9b** and 0.0158 g (0.168 mmol) of norbornene dissolved in 0.5 mL of C_6D_6 was transferred to an NMR tube. The tube was degassed and flame sealed and heated to 45 °C in the probe of a 400 MHz NMR spectrometer. The reaction was monitored over 2-min intervals. With 27% starting material remaining, the products of the reaction were identified as the dimer $[Cp_2Zr(NTol)]_2$ (39%) and the [2 + 2] cycloaddition product of $Cp_2Zr{=}NTol$ and norbornene (27%) by comparison with spectral data reported earlier.[7]

Reaction with PhN=CHPh (4). A solution containing 0.008 g (0.0020 mmol) of complex **9a** and 0.0038 g (0.0021 mmol) of PhN=CHPh dissolved in 0.5 mL of C_6D_6 was prepared and transferred to an NMR tube. The tube was degassed and flame sealed, and the reaction mixture was heated to 45 °C. After 30 min, the ^1H NMR spectrum of the violet solution was taken, and the product was identified as diazametallacycle **3**: yield 85%. Similar reactions carried out with **9b** and **10b** also give diazametallacycle products.

Thermolysis of 10a. A bomb was charged with a solution that contained 0.013 (0.030 mmol) of **10a** dissolved in benzene (5 mL). It was heated to 135 °C for 1 h. Upon cooling the green crystalline dimer product formed. It was isolated by filtration (0.0088 g, 97%). Similar result were obtained when **9a** was subjected to thermolysis at 70 °C.

$Cp_2Zr(N(t\text{-}Bu)N{=}NC(Me){=}C(Me)N(Ph))$ (13). An amount of **3a** (0.0630 g; 0.153 mmol) was dissolved in 5 mL of benzene, and an excess of 2-butyne (100 μL) was added to the mixture. The reaction mixture was transferred to a bomb, degassed, sealed, and was then heated to 45 °C for 45 min. During this time the solution color turned from purple to brown. The solvent was evaporated under vacuum and a brown residue was obtained. It was dissolved in a minimum of pentane solvent and cooled to −40 °C to give a brown microcrystalline product: yield 0.0485 g (68%); IR (C_6H_6) 2968, 2931, 1602, 1433, 1365, 1290, 1159, 1074, 791, 754 cm^{-1}; ^1H NMR (400 MHz, C_6D_6) δ 1.31 (s, 9H, $C(CH_3)_3$), 1.67 (s, 3H, CH_3), 2.12 (s, 3H, CH_3), 5.81 (s, 10H, C_5H_5), 6.67 (d, J_{HH} = *7.25 Hz*, 2H, C-*H*), 6.93 (t, J_{HH} = 7.4 Hz, 1H, C-*H*), 7.19 (t, J_{HH} = 7.4 Hz, 2H, C-*H*); $^{13}C\{^1H\}$ NMR (400 MHz, C_6D_6) δ 14.2 (CH_3), 15.8 (CH_3), 29.0 ($C(CH_3)_3$), 60.2 ($C(CH_3)_3$), 108.5 (C_5H_5), 112.8 (*C*-H), 121.4 (*C*-H), 124.2 (*C*-H), 128.3 (*C*-H). Anal. Calcd for $C_{24}H_{30}N_4Zr$: C, 61.89, H, 6.49, N, 12.03. Found: C, 61.86; H, 6.88; N, 12.09.

$Cp_2Zr(N(Tol)N{=}NC(Me){=}C(Me)N(Tol))$ (14). A solution containing 0.0388 g (0.0844 mmol) of **10b** dissolved in 10 mL of benzene and an excess of 2-butyne (100 μL) was placed in a reaction bomb. The bomb was removed from the drybox and placed on a vacuum line where it was degassed. The green reaction mixture was heated to 135 °C in an oil bath for 30 min, and, after heating, the solution color was deep blue. This mixture was returned to the drybox, and the solvent was removed under vacuum to give a blue solid. It was recrystallized from toluene layered with pentane at −40 °C (yield 0.0280 g; 65%): IR (C_6D_6) 3101, 3045, 2372, 2333, 1965, 1826, 1485, 1227, 1134, 1132, 683 cm^{-1}; ^1H NMR (400 MHz, C_6D_6) δ 1.71 (s, 3H, CH_3), 2.21 (s, 3H, Tol CH_3), 2.22 (s, 3H, Tol CH_3), 2.30 (s, 3H, CH_3), 5.90 (s, 10H, C_5H_5), 6.67 (d, J_{HH} = 8.0 Hz, 2H, C-*H*), 6.98 (d, J_{HH} = 8.0 Hz, 2H, C-*H*), 7.18 (d, J_{HH} = 8.0 Hz, 2H, C-*H*), 7.26 (d, J_{HH} = 8.0 Hz, 4H, C-*H*); $^{13}C\{^1H\}$ NMR (MHz, C_6D_6) δ 20.6 (CH_3), 112.5 (C_5H_5), 118.3 (*C*-H), 128.3 (*C*-H), 129.2 (*C*-H), 131.9 (*C*-H). Anal. Calcd for $C_{24}H_{24}N_4Zr$: C, 65.46, H, 5.89, N, 10.90. Found: C, 63.10; H, 5.89; N, 10.01. Repeated analyses failed to improve the carbon value.

Crystal Structure Determination for 14. Blue blocklike crystals of **14** were obtained by slow cooling of a toluene solution layered with pentane to −40 °C. A crystal structure determination was carried out as described earlier with the following changes. The crystal was cooled to −95 °C, and 3213 raw intensity data were collected. The cell parameters and specific data collection parameters for this data set are given in Tables 4 and 5. Inspection of the intensity standards revealed that no correction for crystal decay was necessary. Space group $P2_1/n$ was confirmed by refinement. The structure was solved by Patterson methods and refined via standard least-squares and Fourier techniques. Inspection of the azimuthal scan data showed a variation of I_{min}/I_{max} = 0.933. The final residuals for 138 variables refined against the 1720 data set for which $F^2 > 3\sigma(F^2)$ were R = 7.2 %, wR = 8.3%, and GOF = 2.43. The R value for all 2861 data was 13.6%. The largest peak in the final difference Fourier map had an electron density of 0.67 e^-/A^3 and the lowest excursion −0.41 e^-/A^3. The p-factor, used to reduce the weight of intense reflections, was set to 0.03 in the last cycles of refinement. Positional parameters with isotropic thermal parameters and anisotropic thermal parameters are provided in the supplementary material.

$Cp_2Zr(N(Tol)N{=}NC(Me){=}C(Ph)N(Ar))$ (15). A solution containing 0.0059 g (0.0013 mmol) of $Cp_2Zr(N(Ar)C(Ph){=}C(Me))$ and 1 equiv of $TolN_3$ (0.0020 g, 0.0015 mmol) dissolved in 10 mL of benzene was stirred for 15 min at room temperature. The solvent was removed under vacuum to give a blue solid. It was recrystallized from pentane at −40 °C (yield 0.0030 g; 38%). IR (C_5H_{12}) 1589, 1558, 1504, 1292, 1236, 1173, 876, 806, 696 cm^{-1}; ^1H NMR (400 MHz, C_6D_6) δ 1.59 (s, 3H, CH_3), 2.18 (s, 6H, CH_3), 2.21 (s, 3H, CH_3), 5.85 (s, 10H, C_5H_5), 6.72 (dd, J_{HH} = 15.9, 8.0 Hz, 1H, C-*H*), 6.96 (t, J_{HH} = 7.7 Hz, 2H, C-*H*), 7.01 (d, J_{HH} = 7.3 Hz, 2H, C-*H*), 7.09 (d, J_{HH} = 8.4 Hz, 2H, C-*H*), 7.21 (d, J_{HH} = 8.4 Hz, 2H, C-*H*), 7.31 (t, J_{HH} = 7.7 Hz, 2H, C-*H*), 7.57 (d, J_{HH} = 7.1 Hz, 2H, C-*H*); $^{13}C\{^1H\}$ NMR (MHz, C_6D_6) δ 20.5 (CH_3), 111.3 (*C*-H), 111.6 (C_5H_5), 116 (*C*-H), 128.2 (*C*-H), 129.6 (*C*-H), 135 (*C*-H).

Acknowledgment. We are grateful to Dr. Frederick Hollander for solving the crystal structures of **8** and **14** and to the National Institutes of Health for financial support (Grant. No. R37 GM-25459). We also acknowledge Dr. William Nugent (E. I. DuPont de Nemours and Co.) for a thoughtful suggestion regarding our kinetic analysis and J. L. Polse and Dr. G. Ball for their assistance with NOESY and low temperature NMR experiments.

Supplementary Material Available: Additional structural data for complexes **8** and **14** (6 pages). This material is contained in many libraries on microfiche, immediately follows this article in the microfilm version of the journal, and can be ordered from the ACS; see any current masthead page for ordering information.

JA942904O